magnetic measurement of ξ via Eq. (15). (See note added in proof.)

In view of the above conclusions, the Bi data are a puzzle: The τ_0 value and the τ^{-1} dependence agree well with the AL predictions, whereas the effects of strong coupling and three-dimensionality are not observed. This circumstance, along wlth the large τ_0 values observed in Al,[4,6] indicates that quantitative discrepancies with the AL theory occur in other materials.

In conclusion, we believe that the present data and analysis cast serious doubt on the validity of previous experimental verification of the AL theory. Until a consistent and verifiable explanation can be given of the various discrepancies discussed above, we must conclude that the previously reported agreement between experiment and theory is, at least in part, fortuitous.

Note added in proof. It has been pointed out to us by Dr. R. S. Thompson that the structure of the films may be such that the mean free path, and therefore the coherence length ξ, is anisotropic. In that case, the ξ relevant for the function G in Eq. (2) might be different from that measured by perpendicular fields [Eq. (15)]. This possibility may be investigated, however, by performing parallel and perpendicular critical field measurements near T_c, and checking the agreement with the GLAG theory.

ACKNOWLEDGMENTS

We are deeply indebted to P. A. Turner, who performed the electron-microscope studies and provided us with clarifying discussions of film growth behavior. J. J. Hauser stimulated many helpful discussions of superconducting thin films and, in particular, of the field effects. Finally, we would like to acknowledge informative conversations and correspondence with R. E. Glover, T. M. Rice, B. I. Halperin, and H. Schmidt.

PHYSICAL REVIEW VOLUME 181, NUMBER 2 10 MAY 1969

Spin Motions in a Classical Ferromagnet*

R. E. WATSON, M. BLUME, AND G. H. VINEYARD
Brookhaven National Laboratory, Upton, New York
(Received 17 January 1969)

The static and dynamic behavior of a simple cubic lattice of classical spins with Heisenberg interactions has been examined by computer on arrays of up to 8192 spins with periodic boundary conditions. Equilibrium values of the energy and magnetization at various temperatures are obtained by Monte Carlo calculations. The results indicate that the magnetization is well approximated by the formula $(1-T/T_c)^\beta$, with $0.32\lesssim\beta\lesssim0.36$ for the full range of temperature from zero to the Curie point T_c. Spin arrays whose energy and magnetization agree with the ensemble averages at a given temperature are taken as characteristic of that temperature. These are then employed to obtain instantaneous and time-displaced spin-correlation functions, the latter involving the numerical solution of the equations of motion of the spin system. The time-displaced correlations show considerable structure. For the most part, spin-wave theory agrees with the low-temperature results. Raising the temperature slows down and smears the structure of the time-displaced correlations. The slowing is much less pronounced than the drop in magnetization. The pulse emanating from a single misaligned spin in a lattice at zero temperature is also calculated.

I. INTRODUCTION

THE statistical mechanical properties of the three-dimensional Heisenberg ferromagnet have been studied by a variety of mathematical techniques, but no exact solutions exist. Some of the properties, such as magnetization and Curie temperature, are better understood than others. In particular, the dynamical behavior of the spin system, except in the spin-wave region, is not known in any detail. Since this dynamical behavior determines the scattering and resonance properties of magnetic materials, it is desirable to obtain a better picture.

Ideally, one would like to study the properties of a system governed by the Hamiltonian

$$\mathcal{H}=-\tfrac{1}{2}\sum_{mn}J(m-n)\mathbf{S}^m\cdot\mathbf{S}^n-g\mu\mathbf{H}\cdot\sum_m\mathbf{S}^m, \qquad (1)$$

where the quantities $\mathbf{S}^m$ are quantum-mechanical spin operators satisfying the usual commutation relations for angular momenta. Such systems, or close approximations thereto, are found in nature, examples being the ferromagnets EuO and EuS, and the antiferromagnet $RbMnF_3$. The Weiss molecular-field approximation[1] provides a qualitative guide to the occurrence of spontaneous magnetization, and series expansion studies and Padé approximant extrapolations[2] based on these expansions yield more refined results for the magnetization. Further, Green's-function analysis[3] has

* Work performed under the auspices of the U. S. Atomic Energy Commission.

[1] See, e.g., C. Kittel, *Introduction to Solid State Physics* (Wiley-Interscience, Inc., New York, 1956), 2nd ed., p. 402.

[2] G. A. Baker, *Advances in Theoretical Physics* (Academic Press Inc., New York, 1965), Vol. 1, p. 1.

[3] D. N. Zubarev, Usp. Fiz. Nauk **71**, 71 (1960) [English transl.: Soviet Phys.—Usp. **3**, 320 (1960)].

yielded information about the dynamical properties of a Heisenberg ferromagnet as well as the static properties. The quantities of interest are the spontaneous magnetization per ion (taken in the z direction)

$$\mathbf{M}=\lim_{H\to 0} g\mu\langle S_z{}^n\rangle=\lim_{H\to 0} g\mu\ \mathrm{Tr}(e^{-\beta\mathfrak{IC}}S_z{}^n)/\mathrm{Tr}(e^{-\beta\mathfrak{IC}}), \quad (2)$$

the energy

$$E=\langle\mathfrak{IC}\rangle, \quad (3)$$

and the time-dependent correlation functions

$$\langle S_\alpha{}^n(0)S_\beta{}^m(t)\rangle,$$

where $\alpha, \beta = x, y, z$ and

$$S_\beta{}^m(t)=e^{i\mathfrak{IC}t/\hbar}S_\beta{}^m(0)e^{-i\mathfrak{IC}t/\hbar}.$$

These are all more or less directly determined from experiment, and a theory of these quantities as a function of temperature would provide a description of the ferromagnetic-paramagnetic phase transition.

In this paper we consider a different approach to the calculation of these quantities, i.e., a computer simulation of a system governed by the Hamiltonian (1). This type of "theoretical experiment" has been performed on many other systems of interacting particles, including solids undergoing radiation damage[4] and liquids.[5] The results obtained here may be considered as further "experimental" data which can be compared with the results of other analytical approximations, or as "theoretical" numbers to be compared with appropriate experiments.

A preliminary estimate of the computer time and storage required for the evaluation of the magnetization and correlation functions of a system of N spins quickly shows that it is not feasible to attack the quantum-mechanical problem numerically. A quantum state of a system of N spins $\frac{1}{2}$ is specified by 2^N complex numbers.[6] Thus an exact treatment of a system with as few as 20 spins is already prohibitively difficult. We avoid this problem by restricting our consideration to the "classical" Heisenberg model in which the quantities $\mathbf{S}^n$ are assumed to be ordinary unit vectors rather than quantum-mechanical operators. We then require only $2N$ numbers to specify the state of the system at any time. These may be chosen as the azimuthal and polar angles of each of the individual spins. The classical model has been considered by a number of authors and there is a considerable literature on the subject.[7–9] One expects that properties of the quantum-mechanical Heisenberg model will approach those of the classical model as the magnitude S of the quantum spins becomes large.

We present here the results of a computer study in which we have determined numerically the magnetization, the energy, and the space- and time-dependent spin-correlation functions. These calculations involve the numerical solution of the equations of motion for a finite three-dimensional simple cubic array of up to 8192 classical spins. As is described in detail in a later section, Monte Carlo techniques have been used to provide an ensemble of arrays of spins characteristic of a given temperature. The equations of motion are then solved using one of these arrays as an initial configuration. A by-product of the Monte Carlo calculations is the dependence of energy and magnetization upon temperature.

In Sec. II we consider the model in detail and outline the strategy of the computation. Section III presents the analytic results available from the spin-wave approximation. Section IV contains numerical results for time-independent properties of the system, such as energy and magnetization, obtained directly from the Monte Carlo calculations. The techniques used in evaluating these quantities are, as discussed in Sec. II, poorly convergent in the region of the Curie temperature for the very reason that this region is of interest, i.e., because of the large critical fluctuations. We are nevertheless able to fit the magnetization curve to a law of the form $M=(1-T/T_c)^\beta$, with $\beta\approx 0.32$–0.36. This law appears to hold down to $T=0$! In Secs. IV and V we discuss the instantaneous and time-displaced correlations, respectively. The results are stable to changes in array size and choice. There is considerable structure (as a function of time) in the time-displaced correlations. This structure is also predicted, for the low-temperature results, by spin-wave theory and is both slowed down and smeared as the temperature is raised. One may explicitly observe the evolution of a spin array in time as an alternative to obtaining $\langle\mathbf{S}^n(0)\cdot\mathbf{S}^m(t)\rangle$. Moving pictures have been obtained in this way and we display stills from these pictures in Sec. V to demonstrate the disturbance emanating from a single misaligned spin.

II. MODEL AND METHOD OF CALCULATION

We consider the classical Heisenberg model of a ferromagnet in which each site n of a simple cubic lattice is occupied by a spin $\mathbf{S}^n$. The spins are ordinary three-dimensional unit vectors, and they interact with an energy $-J(n-m)\mathbf{S}^m\cdot\mathbf{S}^n$. The Hamiltonian of the system is then given by Eq. (1), with the external magnetic field set equal to zero. The equations of

[4] J. B. Gibson, A. N. Goland, M. Milgram, and G. H. Vineyard, Phys. Rev. **120**, 1229 (1960).

[5] B. J. Alder and T. E. Wainwright, J. Chem. Phys. **31**, 459 (1960); A. Rahman, Phys. Rev. **A134**, 246 (1964); A. Paskin, Advan. Phys. **16**, 223 (1967).

[6] This is seen by expanding the state in a basis in which the z component of each individual spin is diagonal. There are 2^N such states.

[7] H. A. Brown and J. M. Luttinger, Phys. Rev. **100**, 685 (1955); M. E. Fisher, Am. J. Phys. **32**, 343 (1964); G. S. Joyce, Phys. Rev. **155**, 478 (1967).

[8] P. J. Wood and G. S. Rushbrooke, Phys. Rev. Letters **17**, 307 (1966).

[9] H. E. Stanley and T. A. Kaplan, Phys. Rev. Letters **16**, 981 (1966).

motion for these classical spins are taken to be[10]

$$\frac{d\mathbf{S}^n}{dt}=-[\sum_m J(n-m)\mathbf{S}^m]\times\mathbf{S}^n. \quad (4)$$

We restrict our attention to nearest-neighbor interactions, i.e.,

$$J(n-m)=J=1, \quad m \text{ and } n \text{ nearest neighbors}$$
$$=0, \quad \text{otherwise}.$$

It follows from the equations of motion (4) that the Hamiltonian $\mathcal{H}$, the magnitude $|\mathbf{S}^n|$ of each spin, and the total magnetization of the system

$$\mathbf{M}=g\mu\sum_{n=1}^{N}\mathbf{S}_n$$

are all conserved in the absence of an external field, i.e.,

$$\frac{d\mathbf{M}}{dt}=\frac{d|\mathbf{S}^n|}{dt}=\frac{d\mathcal{H}}{dt}=0.$$

Since the equations of motion are of first order, specification of the directions of the spins at any one time determines the spins at all other times.

In brief, the computer simulation of this system consists of the selection, by Monte Carlo techniques, of an ensemble of spin arrays characteristic of a given temperature. The equations of motion are next solved numerically, using one of these arrays as an initial configuration. The time-displaced correlation functions are evaluated from the time evolution of this single array, while the Monte Carlo calculations yield the dependence of energy and magnetization on temperature.

We may now consider in more detail the procedures involved in the calculation. We describe separately the boundary conditions, the Monte Carlo techniques, and the numerical solution of the equations of motion.

A. Boundary Conditions

All of the calculations have been performed for simple cubic lattices in the form of a rectangular parallelopiped with periodic boundary conditions. For computational convenience these conditions are of the "staggered" type, so that the spin at the end of one row is equivalent to the spin at the beginning of the next row, rather than to the one at the beginning of the same row. This enables us to label the spins sequentially, with a single index n, $1\leq n\leq N$. In this scheme, for a simple cubic lattice with ν lattice sites on a side (so that $N=\nu^3$), the nearest neighbors of the nth spin are then $n\pm1$, $n\pm\nu$, $n\pm\nu^2$ (modulo N).

B. Determination of the Static Properties by Monte Carlo Techniques

The Monte Carlo calculation follows the basic idea first proposed by Metropolis *et al.*[11,12] for the determination of the equilibrium properties of an imperfect gas. In effect, we construct an ensemble of spin arrays which approaches the canonical ensemble at a given temperature T for our system. This is accomplished by starting with an arbitrary initial spin array as the first member of the ensemble. A single spin of that initial array is selected at random and its direction is changed at random. The change in energy ΔE produced by the change in direction of that single spin is then calculated. If $\Delta E<0$, the array with changed spin is chosen as the second member of the ensemble. If $\Delta E>0$, we calculate $e^{-\Delta E/kT}$ and compare this with a random number r $(0<r<1)$ found by the computer. If $e^{-\Delta E/kT}>r$, the array with changed spin is still chosen as the second member of the ensemble. Otherwise, the initial array is taken as the second member. This procedure is then repeated on the second member in order to choose the third, etc. The result of this procedure is in the limit, as shown by Metropolis *et al.*,[11] an ensemble distributed canonically. On the CDC 6600 computer which was used in our calculations, 10^6 of the steps described above take 9 min. The energy and magnetization are obtained by calculating these quantities for each member of the ensemble and averaging. In practice, we calculate the rms magnetization rather than the magnetization itself, since the latter quantity will average to zero in the absence of an external magnetic field.

C. Numerical Solution of Equations of Motion

The Monte Carlo calculation enables us to find an array whose energy and magnetization lie very close to the most probable energy and magnetization at a given temperature. We then choose arbitrarily a *single* such array to use as the initial configuration. From this starting configuration, the causal evolution in time of the system is governed by the classical equations of motion (4). The numerical integration of these equations is accomplished by a stepwise method. Equation (4) requires that the spin $\mathbf{S}^n(t)$ be instantaneously pre-

[10] Strictly speaking, these are classical equations of motion in only a special sense. They have been derived from the quantum-mechanical equations of motion $d\mathbf{S}_n/dt=(i/\hbar)[\mathcal{H},\mathbf{S}_n]$, with $\mathcal{H}$ given by (1), by performing the commutation on the right and then replacing operators by corresponding classical variables. [It is well known that this procedure is correct in the limit of large quantum spins S; see M. E. Fisher, Am. J. Phys. 32, 343 (1964), for a discussion of this point.] They are not the equations of motion of any ordinary classical gyroscopic system, however, because they lack inertial terms that arise from the kinetic-energy part of a classical Hamiltonian (unless the assumption is made that the moments of inertia about axes perpendicular to the symmetry axis are zero, or that the angular velocity about the symmetry axis is made to approach infinity). Since finite spins are intrinsically nonclassical, the choice of a classical approximation to them is somewhat arbitrary. The present choice is formally and computationally the simplest.

[11] N. Metropolis, A. W. Rosenbluth, M. N. Rosenbluth, A. H. Teller, and E. Teller, J. Chem. Phys. 21, 1087 (1953).

[12] L. D. Fosdick, *Methods in Computational Physics* (Academic Press Inc., New York, 1963), Vol. 1, p. 245.

cessing about the direction of the effective field

$$\mathbf{H}_n^*(t) = -\sum_m J(n-m)\mathbf{S}^m(t) \tag{5}$$

with the instantaneous angular velocity $H_n^*(t)$. Given the two sets of spins $\mathbf{S}^n(t-\Delta t)$ and $\mathbf{S}^n(t)$, $\mathbf{H}_n^*(t)$ is calculated from (5) and $\mathbf{S}^n(t+\Delta t)$ is then formed by rotating the vector $\mathbf{S}^n(t-\Delta t)$ about $\mathbf{H}_n^*(t)$ through the angle $\mathbf{H}_n^*(t)2\Delta t$. Each spin is updated in this fashion and the process is iterated. Exact conservation of magnitude of each spin is thus assured. To start the process at $t=0$ from an initial array of spins, a slight departure from this procedure was used. $\mathbf{S}^n(0)$ was rotated about $\mathbf{H}_n^*(0)$, instead of $\mathbf{H}_n^*(\Delta t)$, to find $\mathbf{S}^n(\Delta t)$ instead of $\mathbf{S}^n(2\Delta t)$. To minimize error, a smaller time step was used at the start. Following this, the standard procedure was used, except that Δt was doubled each time until the desired standard Δt was reached, after which the integration proceeded in the normal fashion as long as desired. The standard Δt was chosen so that quantities such as $\mathbf{M}$ and E were, in fact, conserved in the course of calculation. The result of this choice was that a typical spin would precess once in a time of about $100\Delta t$.

The correlation functions are found by calculating the quantities $\langle S_\alpha^n(0)S_\beta^{n+\Delta n}(t)\rangle$. The averages are performed in this case over the sites n and over equivalent Δn. The correlation functions are thus evaluated from calculations with a single array, while the magnetization and energy are evaluated using ensemble averages. For large enough arrays, the difference should be negligible.

The Monte Carlo procedure for finding an initial array is necessitated by the fact that in this model there are two constants of the motion: the energy and the magnetization. It is unlikely that an arbitrarily chosen array of spins will have both energy and magnetization corresponding to equilibrium values at the same temperature. Moreover, while it is straightforward to calculate the energy and the magnetization of any given array of spins, the temperature that corresponds to either is not readily apparent. Note that there is no equipartition theorem for the system, except in the limits of very low or very high temperature, and no general closed expression for the energy or the magnetization is known. Other stratagems for finding equilibrium states by solving for the motion under the influence of extra interactions or artificial heat baths can be imagined, but appear to be more time consuming.

III. SPIN-WAVE PREDICTIONS

In this section we give a short summary of analytical results that may be readily obtained for classical systems through the spin-wave approximation.[13] The magnetization of the system at low temperatures may be obtained from the relations

$$\begin{aligned}\frac{M(T)}{M(0)} &= \langle S_z{}^r\rangle \cong S - \langle a_r{}^\dagger a_r\rangle \\ &= S - \frac{1}{N}\sum_{\mathbf{k},\mathbf{k}'}\langle b_\mathbf{k}{}^\dagger b_{\mathbf{k}'}\rangle e^{(\mathbf{k}-\mathbf{k}')\cdot\mathbf{r}} \\ &= S - \frac{V_0}{(2\pi)^3}\int_{\mathrm{BZ}} n_\mathbf{k} d\mathbf{k}.\end{aligned} \tag{6}$$

The integral is over the Brillouin zone; V_0 is the volume of a unit cell, the a_r's are step-up and step-down spin operators associated with site $\mathbf{r}$, and the $b_\mathbf{k}$'s are spin-wave creation and annihilation operators. The a's and b's are related by

$$a_r(t) = \frac{1}{\sqrt{N}}\sum_\mathbf{k} b_\mathbf{k} e^{i(\mathbf{k}\cdot\mathbf{r}-\omega_\mathbf{k}t)}. \tag{7}$$

Also, $b_\mathbf{k}{}^\dagger b_\mathbf{k} = n_\mathbf{k}$, the spin-wave occupation number. The spin-wave energy $\omega_\mathbf{k}$ for the near-neighbor-coupled simple cubic lattice is

$$\omega_\mathbf{k} = \tfrac{1}{6}\omega_L\{3-\cos k_x-\cos k_y-\cos k_z\}, \tag{8}$$

where

$$\omega_L = 12SJ \equiv 12$$

is the magnon energy at the zone boundary. For the system defined by Eq. (1) with $S=J=V_0=1$, and the classical low-temperature approximation to the spin-wave occupation number ($n_\mathbf{k}\sim kT/\omega_\mathbf{k}$), one obtains

$$\begin{aligned}\frac{M(T)}{M(0)} &\approx 1 - \frac{6kT}{\pi^3\omega_L}\int_0\int\int^\pi \frac{dk_x dk_y dk_z}{3-\cos k_x-\cos k_y-\cos k_z} \\ &= 1-0.2527T.\end{aligned} \tag{9}$$

This result is valid only in a classical system.

The correlation functions may be obtained in much the same way. The $S_x\,S_x$ transverse function is

$$\begin{aligned}&\langle S_x{}^0(0)S_x{}^r(t)\rangle \\ &\quad = \tfrac{1}{2}S\langle[a_0(0)+a_0{}^\dagger(0)][a_r(t)+a_r{}^\dagger(t)]\rangle \\ &\quad = \tfrac{1}{2}S\frac{V_0}{(2\pi)^3}\int_{\mathrm{BZ}} d\mathbf{k}\,\{(n_\mathbf{k}+1)e^{-i(\mathbf{k}\cdot\mathbf{r}-\omega_\mathbf{k}t)} \\ &\qquad\qquad + n_\mathbf{k}e^{i(\mathbf{k}\cdot\mathbf{r}-\omega_\mathbf{k}t)}\} \\ &\quad \approx \frac{kT}{(2\pi)^3}\int_{-\pi}\int\int^\pi \frac{\cos(\mathbf{k}\cdot\mathbf{r}-\omega_\mathbf{k}t)}{\omega_\mathbf{k}} dk_x dk_y dk_z,\end{aligned} \tag{10}$$

which has again been obtained for the simple cubic lattice, where we have again taken $n_\mathbf{k}\approx n_\mathbf{k}+1\approx kT/\omega_\mathbf{k}$. Thus the instantaneous self-correlation function is

$$\begin{aligned}\langle S_x{}^0(0)S_x{}^0(0)\rangle &= 1-M(T)/M(0) \\ &= 0.2527T.\end{aligned} \tag{11}$$

A more convenient form can be found for the time

[13] See also D. L. Huber, Phys. Rev. **146**, 387 (1966).

dependence of the correlations by taking the time derivative

$$\frac{d}{dt}\langle S_x^0(0)S_x^r(t)\rangle$$
$$=\frac{kT}{(2\pi)^3}\int_{-\pi}\int\int^{\pi}\sin(\mathbf{kr}-\omega_k t)dk_x dk_y dk_z$$
$$=-\frac{1}{2i}\frac{kT}{(2\pi)^3}\Bigg[\prod_{i=1}^{3}\Bigg(\int_{-\pi}^{\pi}e^{i(k_i l_i-\frac{1}{3}\tau\cos k_i)}dk_i\Bigg)e^{i\tau}$$
$$-\prod_{i=1}^{3}\Bigg(\int_{-\pi}^{\pi}e^{i(k_i l_i+\frac{1}{3}\tau\cos k_i)}dk_i\Bigg)e^{-i\tau}\Bigg], \quad (12)$$

where $\tau\equiv\frac{1}{2}\omega_L t$. The factoring into products of integrals is allowed by the form of the magnon energy [Eq. (8)]. Performing the integrations in Eq. (12), we obtain

$$\langle S_x^0(0)S_x^r(t)\rangle=\langle S_x^0(0)S_x^r(0)\rangle$$
$$+\frac{2kT}{\omega_L}\int_0^t d\tau\, J_h(\tfrac{1}{3}\tau)J_k(\tfrac{1}{3}\tau)J_l(\tfrac{1}{3}\tau)\varphi_{h+k+l}(\tau), \quad (13)$$

where h, k, and l are the indices of the lattice vector $\mathbf{r}$, the J's are cylindrical Bessel functions, and

$$\begin{aligned}\varphi_{h+k+l}&\equiv\cos\tau, && \text{when } h+k+l-1=0 \pmod 4\\ &\equiv\sin\tau, && \text{when } h+k+l-1=1 \pmod 4\\ &\equiv-\cos\tau, && \text{when } h+k+l-1=2 \pmod 4\\ &\equiv-\sin\tau, && \text{when } h+k+l-1=3 \pmod 4.\end{aligned}$$

Equation (13) will be evaluated when we explore the time dependence of the correlations. The instantaneous correlations will be obtained with Eq. (10) using Monte Carlo integration techniques.

The longitudinal correlation function is similarly

$$\langle S_z^0(0)S_z^r(t)\rangle-M^2$$
$$=\langle[S-a_0^\dagger(0)a_0(0)][S-a_r^\dagger(t)a_r(t)]\rangle-M^2$$
$$=N^{-2}[\sum_{\mathbf{k}}n_{\mathbf{k}}e^{-i(\mathbf{k}\cdot\mathbf{r}-\omega_{\mathbf{k}}t)}][\sum_{\mathbf{q}}(n_{\mathbf{q}}+1)e^{i(\mathbf{q}\cdot\mathbf{r}-\omega_{\mathbf{q}}t)}]$$
$$+O(N^{-1})$$
$$\approx\langle S_x^0(0)S_x^r(t)\rangle^2+\left(\frac{2kT}{\omega_L}\right)^2$$
$$\times\Bigg(\int_0^t d\tau\, J_h(\tfrac{1}{3}\tau)J_k(\tfrac{1}{3}\tau)J_l(\tfrac{1}{3}\tau)\varphi_{h+k+l-1}\Bigg)^2$$
$$+O(N^{-1}). \quad (14)$$

It has a quadratic dependence on temperature, and, being the sum of squares of real quantities (to order N^{-1}), it is everywhere positive. The results of our Monte Carlo and dynamical numerical calculations for longitudinal correlations are all consistent with this requirement.

IV. RESULTS FOR MAGNETIZATION AND ENERGY

We consider first the results of the Monte Carlo calculations for energy and rms magnetization as a function of temperature. The rms magnetization for arrays of 64, 512, 2048, and 8192 spins appears in Fig. 1. On the right of the figure we indicate the expected rms magnetization for the limit $T\to\infty$. This limiting value is equal to $N^{-1/2}$, and goes to zero as the number of spins becomes infinite. We also indicate the value of the Curie temperature as predicted by molecular-field theory and as determined by Wood and Rushbrooke[8] from extrapolated series expansions. The latter number is expected to be very accurate, and is referred to as T_c. It can be seen that the magnetization curves appear to converge on this value as the number of spins is increased.

We have indicated on the magnetization curve for 8192 spins a measure of the uncertainty in the calculations. The cross-hatches represent fluctuations in the ensemble average of rms magnetization obtained from one or several runs at the same temperature. This scatter is largest, as expected, near T_c, where it is associated with the critical fluctuations. The effect of these fluctuations on the averages can be reduced by taking larger samples in the Monte Carlo procedure. In fact, samplings larger by an order of magnitude were taken at temperatures near T_c than in other temperature ranges. The Monte Carlo results were more accurate in our calculations with smaller N, since we were able to take larger samplings (relative to array size).

The curve in Fig. 1, labeled modified molecular field, is simply the ordinary molecular-field result scaled in temperature to the Wood-Rushbrooke T_c. At temperatures just below T_c all of our results lie above this curve, in agreement with previous observations to the effect that molecular-field theory underestimates the magnetization in this temperature region.

In view of the considerable current interest in the

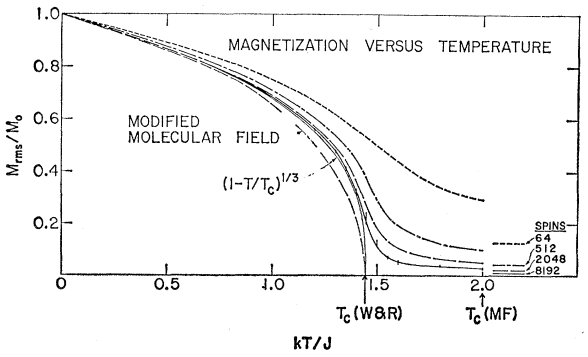

FIG. 1. Root-mean-square magnetization versus temperature from Monte Carlo calculations for various-sized simple cubic arrays. The number of spins in each array and the magnetization at infinite temperature are indicated at lower right.

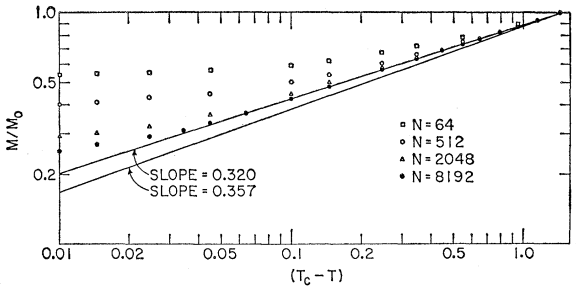

FIG. 2. Log-log plot of rms magnetization versus temperature from Monte Carlo calculations for various-sized arrays. Temperature range is 0–$0.993T_c$. Two sample slopes are also plotted.

power law followed by the magnetization as a function of temperature near T_c, we present a log-log plot of the magnetization curves in Fig. 2. The curves approach a power law of the form

$$M(T)=(1-T/T_c)^{\beta}, \tag{15}$$

with the Wood-Rushbrooke T_c, which appears to hold very closely for the full range of temperature from $T\lesssim T_c$ down to $T=0$. Such a result is not possible at $T=0$ for a quantum spin system, for which $(dM/dT)_0=0$, while Eq. (15) predicts $(dM/dT)_0=-\beta/T_c$. In our classical system, however, $(dM/dT)_0$ is finite and is equal, according to spin-wave theory, to -0.235 for the simple cubic lattice. The straight line through the data in Fig. 2 is drawn with $\beta=0.32$. If we assume that (7) holds down to $T=0$, the spin-wave result, combined with the Wood-Rushbrooke T_c, predicts $\beta=0.365$. We have also shown a plot of $(1-T/T_c)^{1/3}$ in Fig. 1. We conclude that Eq. (15), although not necessarily the exact form, gives an extremely good representation of the magnetization as a function of temperature with $0.32\lesssim\beta\lesssim0.36$. A further test of the form (15) can be made for bcc and fcc lattices for which Wood and Rushbrooke[8] have also given estimates of T_c. We may take the Wood-Rushbrooke T_c, together with $(dM/dT)_0=-\beta/T_c$, and set the latter quantity equal to the low-temperature slope obtained from the spin-wave expansions $M(T)\approx1-\alpha T$ for these lattices. The coefficients α are proportional to the Watson integrals. We then obtain a value of $\beta=\alpha T_c$ for each of the lattices. We find that

$$\beta_{sc}=0.365,$$
$$\beta_{bcc}=0.359,$$
$$\beta_{fcc}=0.356.$$

These values are very close to the value $5/14=0.357$ which has been conjectured by Baker[14] from Padé approximation near T_c (a line of this slope is plotted in Fig. 2). The close agreement between these values leads us to conjecture that T_c is inversely proportional to the Watson integrals for the classical Heisenberg model. The same assumption, in another guise, is that the same initial slope occurs in the magnetization curves for the three lattices when plotted on a reduced temperature scale. If so, the scatter in the above values of β indicates error in the Wood-Rushbrooke values of T_c.

We turn briefly to the results for energy as a function of temperature, which are shown in Fig. 3. The energy per spin follows the same curve irrespective of the number of spins N, except in the vicinity of T_c. We expect that the slope should increase at T_c as N increases, yielding a sharper peak in the specific heat. The scatter in the energy averages is too great to discern any such change of slope, and the envelope of results for all array sizes is indicated in the figure. Much larger Monte Carlo samplings are necessary to obtain useful information near T_c because of large critical fluctuations and because of the inherent difficulty in extracting derivatives from such data.[12]

V. INSTANTANEOUS CORRELATIONS

Instantaneous correlation functions for several temperatures are shown in Fig. 4. These were obtained from the machine calculations; spin-wave predictions will be considered shortly. $\langle S_{11}{}^{r}(0)S_{11}{}^{r+\Delta r}(0)\rangle$ is denoted the "longitudinal" correlation function and refers to components of spin parallel to the magnetization; $\langle \mathbf{S}_{\perp}{}^{r}(0)\cdot\mathbf{S}_{\perp}{}^{r+\Delta r}(0)\rangle$ is the "transverse" correlation function. In calculating the latter quantity we have performed an average over the two components of spin normal to the magnetization. In the figure the scale changes from one plot to the next, and the zero for the longitudinal functions has been taken as $\langle S\rangle^2=(M/M_0)^2$.

The transverse correlation, considered as a function of Δr, is found to have the same shape for all tempera-

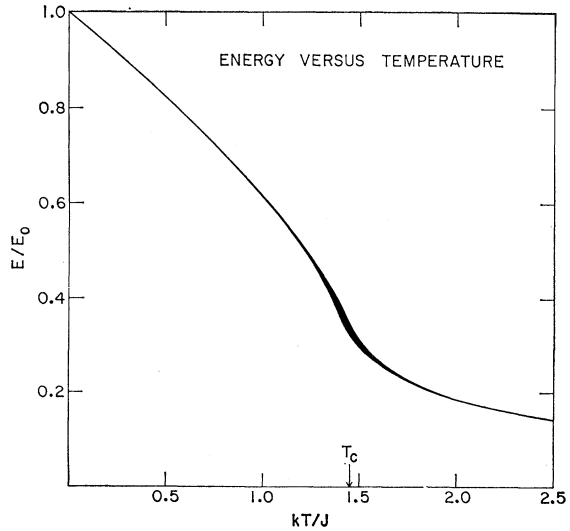

FIG. 3. Energy versus temperature from Monte Carlo calculations. Results for all sizes of arrays, from 46 to 8192 spins, fall within the dark line. The Wood-Rushbrooke value of T_c is indicated.

[14] G. A. Baker (private communication).

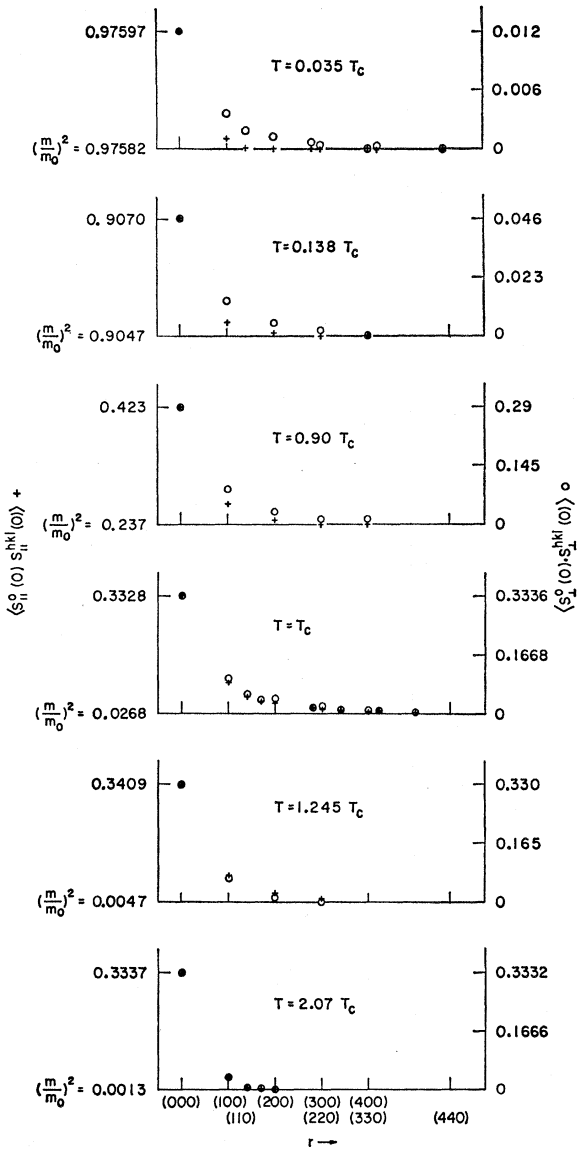

FIG. 4. Instantaneous spin correlations between various neighbors at various temperatures. Longitudinal correlations indicated by crosses (left scale), transverse correlations indicated by open circles (right scale). Note that the scales of the plots vary with temperature.

tures up to T_c, whereas the longitudinal correlation $\langle S_{11}S_{11}\rangle$ contracts as the temperature is lowered below T_c. Both functions become shorter ranged as T increases above T_c.

Various theories yield the asymptotic result

$$\langle \mathbf{S}_i^0(0)\cdot\mathbf{S}_i^r(0)\rangle_T \cong A(T)e^{-\kappa_i(T)r}/r^{1+\eta} \tag{16}$$

in the limit of large r (for example, $\eta=0$ for Ornstein-Zernike theory).[15] The temperature dependence of the range of the spatial distribution is contained in the screening constant $\kappa(T)$. The correlation functions shown in Fig. 4 do not behave like $1/r^{1+\eta}$.

This is not surprising, since our results are for small r and thus do not give a test of asymptotic behavior. Nevertheless, the temperature dependence of the range of the correlation is qualitatively explained by Eq. (16) and the associated behavior for $\kappa(T)$, namely,

$$\kappa_{\perp}(T)=0 \tag{17a}$$

and

$$\kappa_{11}(T)\sim(T_c-T)^{\nu}, \tag{17b}$$

for $T<T_c$. This temperature dependence can be related to that of the magnetic susceptibility implied by Eq. (17):

$$\chi(T)\sim A(T)\kappa(T)^{-2+\eta}. \tag{18}$$

If $A(T)$ is well behaved in the vicinity of T_c, then

$$\nu=\gamma/(2-\eta), \tag{19}$$

where $-\gamma$ is the exponent appropriate to χ. Estimates[16] of γ range between 1 and 2 with a value of $\frac{4}{3}$ favored, while η is normally small (i.e., $\lesssim 0.1$). Thus ν is expected to be about $\frac{2}{3}$. In attempting to generalize Eq. (16) for the region of small r, which is of interest to us here, we might assume the form

$$\langle \mathbf{S}_i^0(0)\cdot\mathbf{S}_i^r(0)\rangle_T = A(T)f(r)e^{-\kappa_i(T)r}, \tag{20}$$

where $f(r)$ is some general, temperature-independent, function of $\mathbf{r}$. An estimate of $\kappa(T)$ may then be obtained from the results of Fig. 4, by taking

$$\kappa_i(T)r=\ln\frac{A(T_c)\langle \mathbf{S}_i^0(0)\cdot\mathbf{S}_i^r(0)\rangle_T}{A(T)\langle \mathbf{S}_i^0(0)\cdot\mathbf{S}_i^r(0)\rangle_{T_c}}. \tag{21}$$

Determining $A(T)$ from the amplitudes of the self-correlation functions, one obtains the $\kappa_i(T)r$ plotted in Fig. 5 for the nearest-neighbor correlation. The scatter is inevitable and comes from estimating an exponent from ratios of "experimental" points. Results for more distant pairs display greater scatter but otherwise are consistent with the results plotted here. The $\kappa_{11}(T)$ for $T<T_c$ suggest a ν which is less than 1 and close to $\frac{2}{3}$. The more rapid temperature dependence of $\kappa(T)$ for $T>T_c$ is also anticipated by most theories. In general, the temperature dependence of the correlation functions, for the range of r values plotted in Fig. 4, is consistent with Eqs. (17) and (20).

The amplitudes $A(T)$ as measured by the self-correlation functions are plotted in Fig. 6. We see[17] that

$$\langle \mathbf{S}_{\perp}^r(0)\cdot\mathbf{S}_{\perp}^{r+\Delta r}(0)\rangle \sim T.$$

Since the fixed length of the spins requires that

$$(M/M_0)^2+2\langle \mathbf{S}_{\perp}^r(0)\cdot\mathbf{S}_{\perp}^r(0)\rangle+\langle S_{11}^r(0)\cdot S_{11}^r(0)\rangle=1, \tag{22}$$

[15] For example, see L. D. Landau and E. M. Lifschitz, *Statistical Physics* (Pergamon Press, Inc., London, 1958), p. 366.

[16] For example, see Ref. 2.

[17] Since our finite samples display a net magnetization above T_c, we can define the longitudinal and transverse functions there as well. There is a distinct tendency for the transverse amplitude to lie higher than the longitudinal.

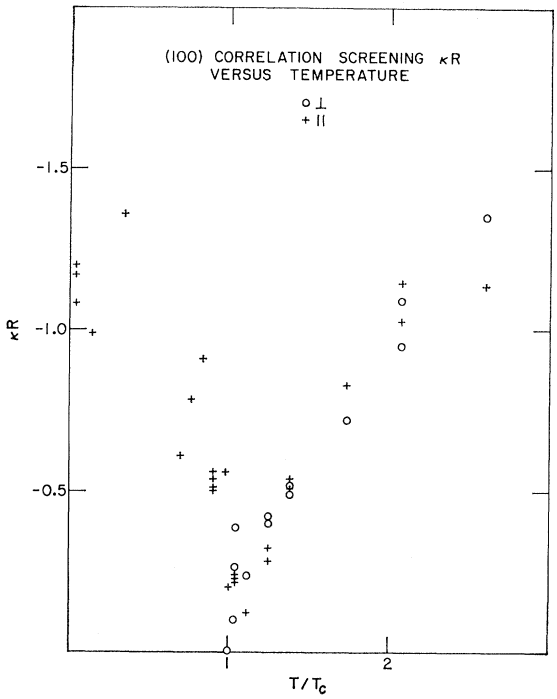

FIG. 5. Screening constant κ for instantaneous correlations of near neighbors versus temperature. Longitudinal correlations, crosses; transverse correlations, open circles. R is the near-neighbor separation. See Eq. (21).

the amplitude of the longitudinal functions $\langle S_{\text{II}} S_{\text{II}} \rangle$ cannot also obey a simple power law in T or $T-T_c$. Spin-wave theory also predicts [see Eq. (12)] that $\langle \mathbf{S}_\perp \cdot \mathbf{S}_\perp \rangle \sim T$, for small T, but gives a larger proportionality constant. This, and the quadratic dependence predicted [see Eq. (15)] for $\langle S_{\text{II}} S_{\text{II}} \rangle$, also appear in Fig. 6. The spin-wave predictions cannot prevail over the full range of temperature (the amplitude at $T=T_c$ would then be greater than $\frac{1}{3}$), and it would seem that the amplitude of $\langle \mathbf{S}_\perp \cdot \mathbf{S}_\perp \rangle$ is only approximately linear in T for the full range $0 \leq T \leq T_c$.

The results reported above were based on arrays of 2048 (16×16×8) spins. It is of interest to compare results for various arrays and to compare these, in turn, with spin-wave predictions. This is done in Fig. 7 for one array of 512, two of 2048, and one of 4096 spins at $T=0.035T_c$. The largest source of scatter among these results is due to small differences in the magnetization, M/M_0, of the chosen samples; the array of 512 spins has the largest M/M_0 and hence tends to lie lowest in the plots [e.g., see Eq. (22)]. There appears to be little significant dependence on the size of the array and, if it were not for the spin-wave predictions, it might seem that results had converged on those appropriate to an infinite-sized sample.[18] The spin-wave results were obtained with Monte Carlo estimates of Eq. (11), and they suggest that the negative values of $\langle \mathbf{S}_\perp^0(0) \cdot \mathbf{S}_\perp^{nnn}(0) \rangle$ (implying antiparallel ordering of the transverse spin components for [*nnn*] pairs) are incorrect. The spin-wave results suggest that one must deal with sample sizes far beyond current computational capabilities in order to predict correctly any but the few nearest-neighbor instantaneous correlation functions. This contrasts with the time dependence of the correlation functions, which is quite well predicted using

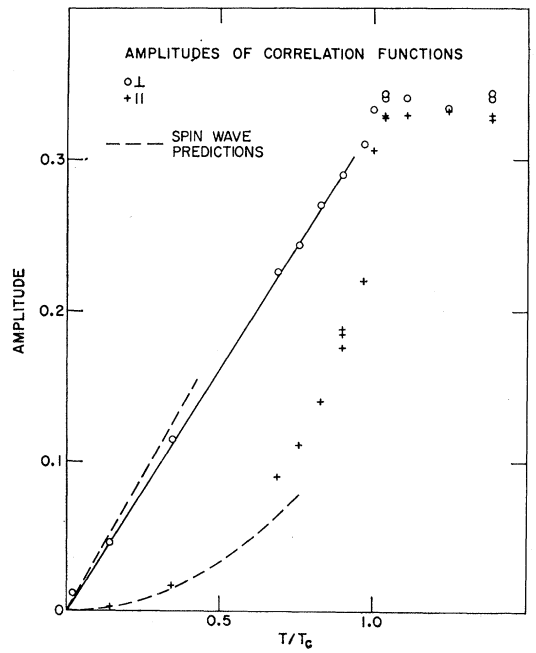

FIG. 6. Amplitude of the instantaneous correlations $A(T)f(0)$ [see Eq. (20)] versus temperature. Low-temperature predictions of spin-wave theory are shown by dotted lines, longitudinal correlations by crosses, and transverse correlations by open circles.

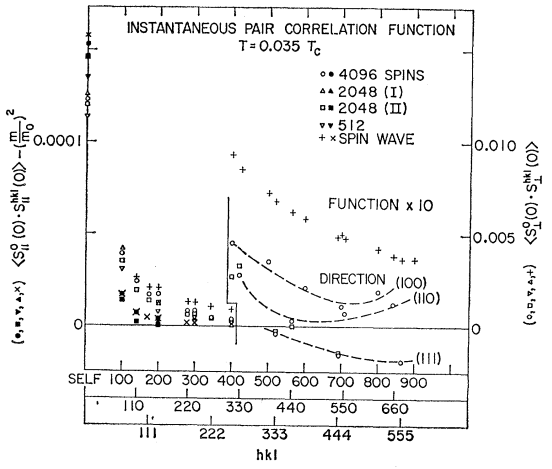

FIG. 7. Instantaneous spin correlations as obtained for several arrays, between various neighbors at temperature $0.035T_c$. Longitudinal correlations on left axis, transverse correlations on right axis. Spin-wave predictions given by × and +. Note the order of magnitude amplification of the right-hand side of the figure.

[18] N. D. Mermin (private communication) reports a proof, consistent with our results, indicating that $\langle S_\perp \cdot S_\perp \rangle$ is positive definite for all [100] pairs in a simple cubic classical Heisenberg ferromagnet.

our sample arrays and the dynamical equations. This will be discussed in Sec. VI.

The spin-wave results yield a slight anisotropy of the sort already suggested by Fig. 4. Fitting the transverse results of Fig. 5 with Eq. (16) (for which $\kappa=0$), one obtains

$$0<\eta<0.17.$$

This range is partially due to the inevitable scatter in fitted values but there is a distinct suggestion that η increases with increasing neighbor distance. The asymptotic behavior has been obtained from spin-wave theory with Eq. (10) for the $[n00]$ direction, yielding $\eta=0$. This would seem to contradict the fitting of Fig. 5, but of course the pairs represented in the figure are far from the asymptotic region.

VI. TIME-DISPLACED CORRELATIONS

One may characterize the time evolution of the spin system by computing the correlation functions, or one may simply inspect the whole array as it moves in time. We will concentrate on correlation functions in this section but we will in one case examine the time evolution of a spin array directly.

Transverse pair correlation functions $\langle \mathbf{S}_\perp(0)\cdot\mathbf{S}_\perp(t)\rangle$ for $T=0.035T_c$ and $N=4096$ are plotted in Fig. 8. As we will shortly see, these can be obtained with greater accuracy than $\langle S_{11}(0)S_{11}(t)\rangle$, and they agree well with the spin-wave predictions. (Note the changes in scale on going to more distant neighbors.) The time unit for τ is the Larmor precession time appropriate to the sample's magnetization [i.e., $\tau^{-1}=3JM/\pi M_0$; see Eq. (5)]. The self-correlation function shows a strong correlation at $\tau=0$ which decays to zero in a time of the order of one Larmor precession, and at larger τ there is an additional peak clearly discernible. The [100] correlation rises to a maximum at $\tau\sim\frac{1}{2}$, i.e., the spins move so that their transverse components are more strongly aligned after one-half a precession time. The [100] peak then decays with the same characteristic time seen for the self-correlation function. For [200] pairs this "main" peak occurs at twice the [100] time. This might be expected since a [200] pair is coupled *via* its [100] intermediary. This would seem characteristic of a "hopping" or "spin-diffusion" velocity and we see the "main" peak move with the same velocity for more distant $[n00]$ pairs. We also see the emergence of other peaks which move with the same velocity and the apparent decline of the "main" peak.

Inspection of the $[nn0]$ and $[nnn]$ correlation functions shows similar behavior. The [110] main peak occurs at twice the [100] time; the [111] peak occurs at thrice the [100] time. This is necessary, since the coupling occurs *via* [100], [010], and [001] near-neighbor pairs. The apparent peak velocity is thus one-half the $[n00]$ for the $[nn0]$ direction and one-third it for the $[nnn]$, but this, in fact, implies a *common* "diffusion" velocity. Whereas no discernible structure appears inside the main peak (i.e., at smaller τ) in the

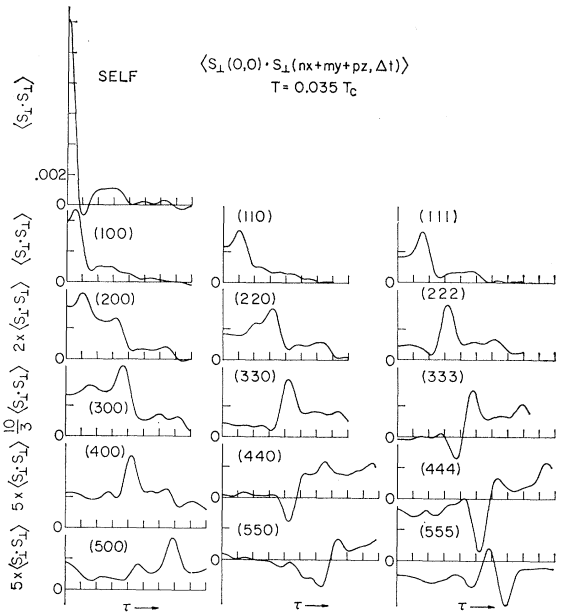

FIG. 8. Transverse time-displaced correlations for various neighbors versus time for a 4096 spin array. τ is time in units of the Larmor precession period defined by the magnetization (see text). $T=0.035T_c$.

$[n00]$ direction, considerable structure appears inside it for the $[nnn]$. In other words, the $[nnn]$ direction shows structures for times less than that appropriate for a signal communicated via a common spin-diffusion velocity. This is surprising and of some interest, and we will return to this matter at the end of this section.

Some feeling of the reproducibility of the correlation functions is given in Fig. 9, where the self- and [200] transverse correlation functions are plotted for different initial arrays (again for $T=0.035T_c$). Results for samples of 512, 2048, and 4096 spins are seen. The two 2048-spin samples were gathered independently in the course of taking the Monte Carlo averages. The different intercepts at $\tau=0$ for the self-correlation function reflect the fact that the samples do not have identical magnetization. These plots suggest that the basic peak structure seen in Fig. 8 is real and not an artifact of sample size or choice. The spin-wave predictions plotted in Fig. 10 indicate that this structure is indeed real. Granting the reality of the peak structure, there is considerable uncertainty attached to quantitative details.

Another way to sample the "noise" of the problem is to take a given spin array, let it evolve in time, and let different times be taken as $\tau=0$ for the purpose of evaluating the correlation function. This is done for both the longitudinal and the transverse [100] function, at $T=0.035T_c$, in Fig. 10. The plots indicate why we concentrate on the transverse functions in this section. Employing different spin array times as $\tau=0$, and evaluating the correlation function, yields results which agree within the width of the plotted line for the transverse function. On the other hand, considerable

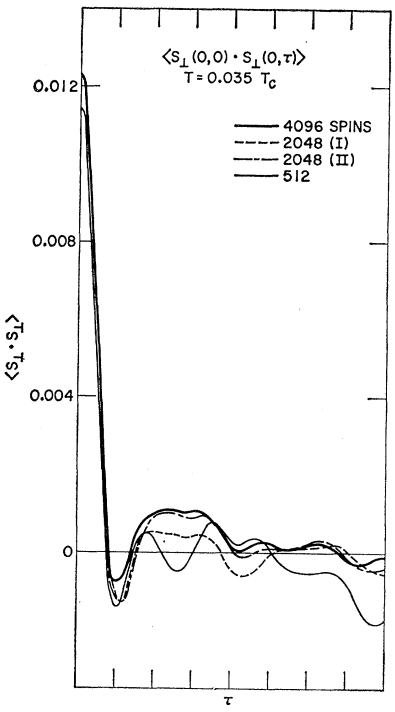

(a)

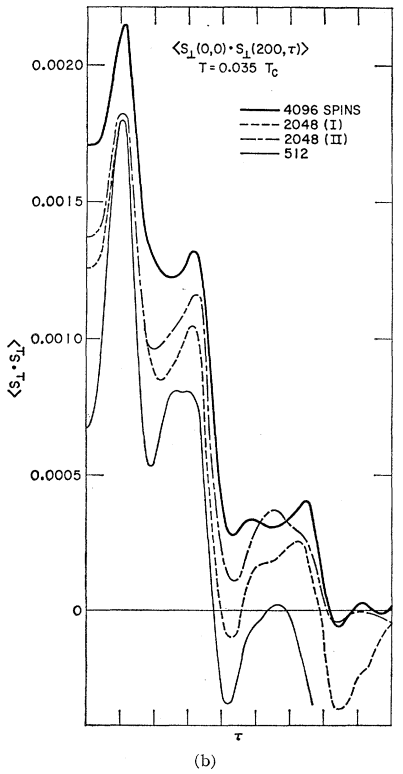

(b)

FIG. 9. Transverse displaced (a) self- and (b) [200]-neighbor correlations versus reduced time at $T=0.035T_c$ for arrays of varying size.

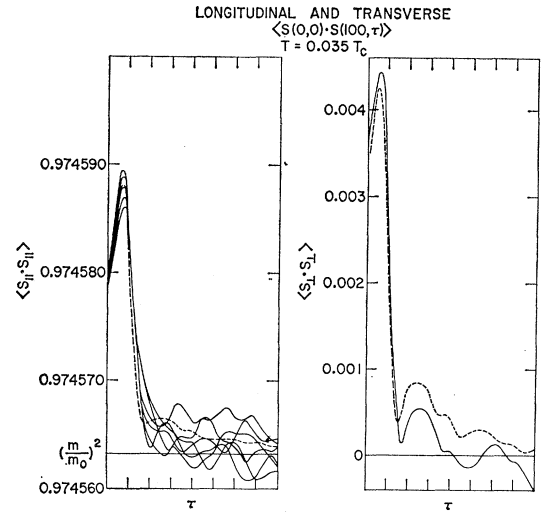

FIG. 10. Longitudinal and transverse time-displaced [100]-neighbor correlations versus reduced time where different times in the array's time evolution were taken as $\tau=0$. $T=0.035T_c$. Low-temperature spin-wave predictions are indicated by the dashed lines; the $\tau=0$ values were chosen arbitrarily and the time evolution obtained by evaluation of the integrals appearing in Eqs. (13) and (14). (The $\tau=0$ choice affects only the vertical position of the transverse spin-wave predictions but does affect the shape of the predicted longitudinal correlation.)

noise is obtained for the longitudinal function. Its *relative* importance is due to the fact that the amplitude [measured with respect to $(M/M_0)^2$] of the longitudinal function is two orders of magnitude smaller than its transverse counterpart. Similar results are plotted for a higher temperature in Fig. 11. The "thermal" scatter is now discernible in the transverse function. Otherwise,

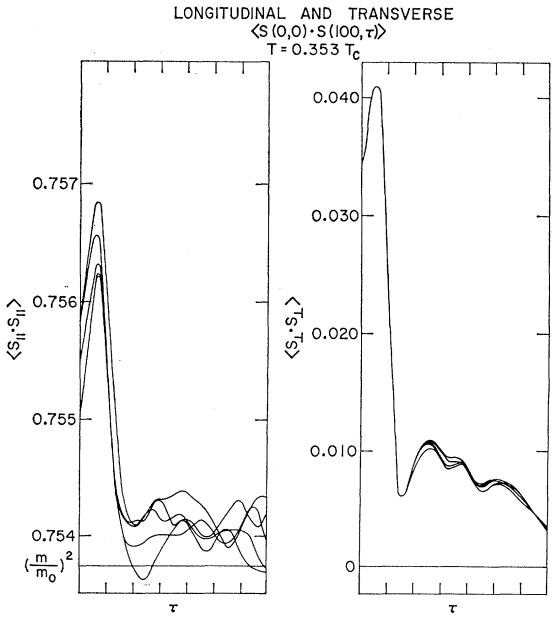

FIG. 11. Longitudinal and transverse spin correlations identical to those depicted in Fig. 10 but for $T=0.353T_c$, with the reduced time unit τ scaled accordingly (see text).

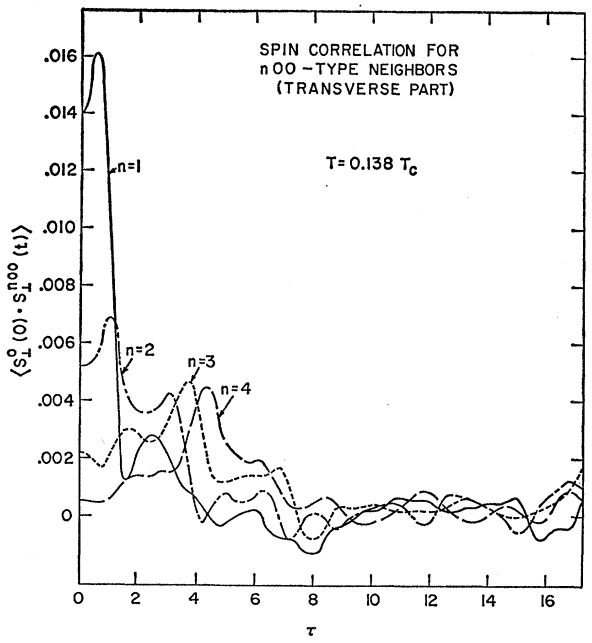

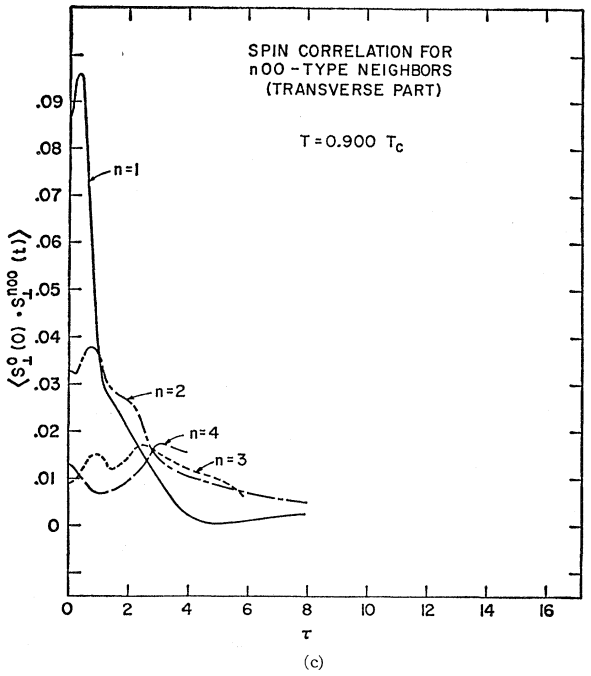

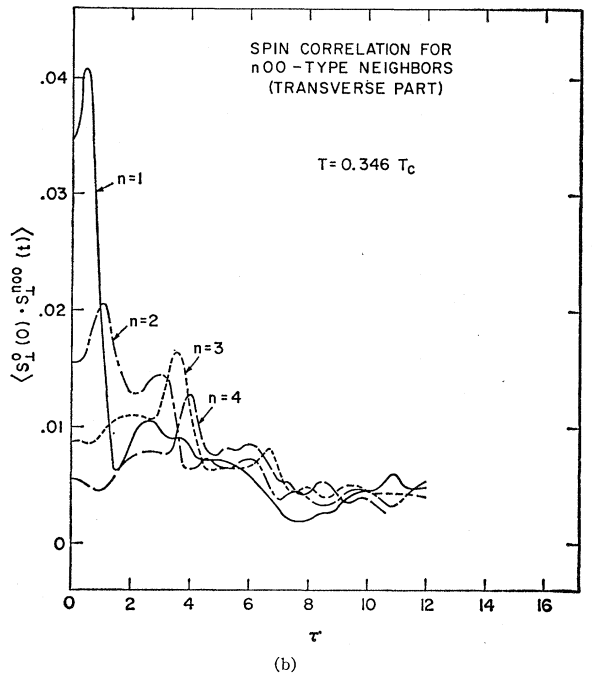

FIG. 12. Transverse, [n00]-neighbor, time-displaced correlations for $T=0.138$, 0.346, and $0.099T_c$ obtained for 2048 spin arrays. The reduced time scales τ vary with values appropriate to $M(T)/M_0$ at the three temperatures. Vertical scales also vary.

it displays structure similar to that seen at the lower temperature.[19] The noise has increased for the longitudinal function but the increase in the function's amplitude causes the *relative* noise to remain almost unchanged. The relative noise increases with further increases in temperature for both correlation functions.

Figure 10 also displays the predictions of spin-wave theory. Equations (14) and (15) were evaluated for the time dependence, and the instantaneous correlations $\langle \mathbf{S}_i^0(0)\cdot\mathbf{S}_i^r(0)\rangle$ were separately scaled so as to match the dynamical plots at the origin. This scaling affects not only the vertical position of $\langle \mathbf{S}_\perp\cdot\mathbf{S}_\perp\rangle$ but also the shape of $\langle S_\parallel S_\parallel\rangle$, as can be seen from Eq. (14). Granting this, the agreement is excellent and, apart from the choice of the simultaneous correlation $\langle \mathbf{S}_\perp^0(0)\cdot\mathbf{S}_\perp^r(0)\rangle$, *all* the results of Fig. 8 are in good agreement with spin-wave theory. It thus seems best to think of the

[19] Here, as elsewhere in this paper, $\langle \mathbf{S}_\perp\cdot\mathbf{S}_\perp\rangle$ is an average of the $\langle S_xS_x\rangle$ and $\langle S_yS_y\rangle$ correlation functions. While $\langle \mathbf{S}_\perp\cdot\mathbf{S}_\perp\rangle$ is quite reproducible, the x-x or y-y term alone is not.

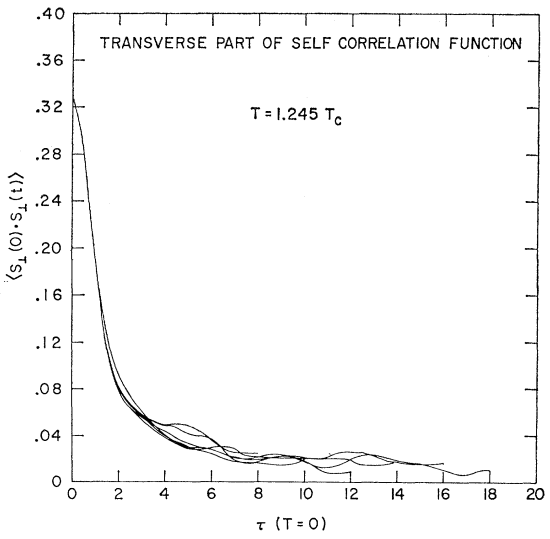

FIG. 13. Transverse time-displaced self-correlation function at $T=1.245T_c$. Different times in the evolution of the array were taken as $\tau=0$. The time scale is the Larmor precession time appropriate to the fully magnetized system at $T=0$.

structure in terms of spin-wave propagation rather than in terms of a diffusion process dominated by a characteristic velocity.

The temperature dependence of the transverse correlation functions is better seen in Fig. 12, where $[n00]$ pair results are shown for $T=0.138$, 0.346, and $0.900T_c$. The correlation functions have slowed down considerably at the higher temperatures, but when plotted as a function of the Larmor precession time τ, they appear to have speeded up slightly. In other words, the time dependence scales well with a precession time defined by the average magnetization with a slight speed up at higher temperatures. This seems due to a local precession time defined by a local magnetization which exceeds the average value for the lattice as a whole. The structure of the correlation functions becomes increasingly smeared with increasing temperature. This is, in part, associated[20] with "thermal noise" of the sort seen in Figs. 10 and 11. The results at $T=0.9T_c$ are quite inaccurate because of this "noise" and could not be resolved for times later than shown.

The transverse self-correlation function, for a temperature above T_c, is plotted in Fig. 13. The time scale

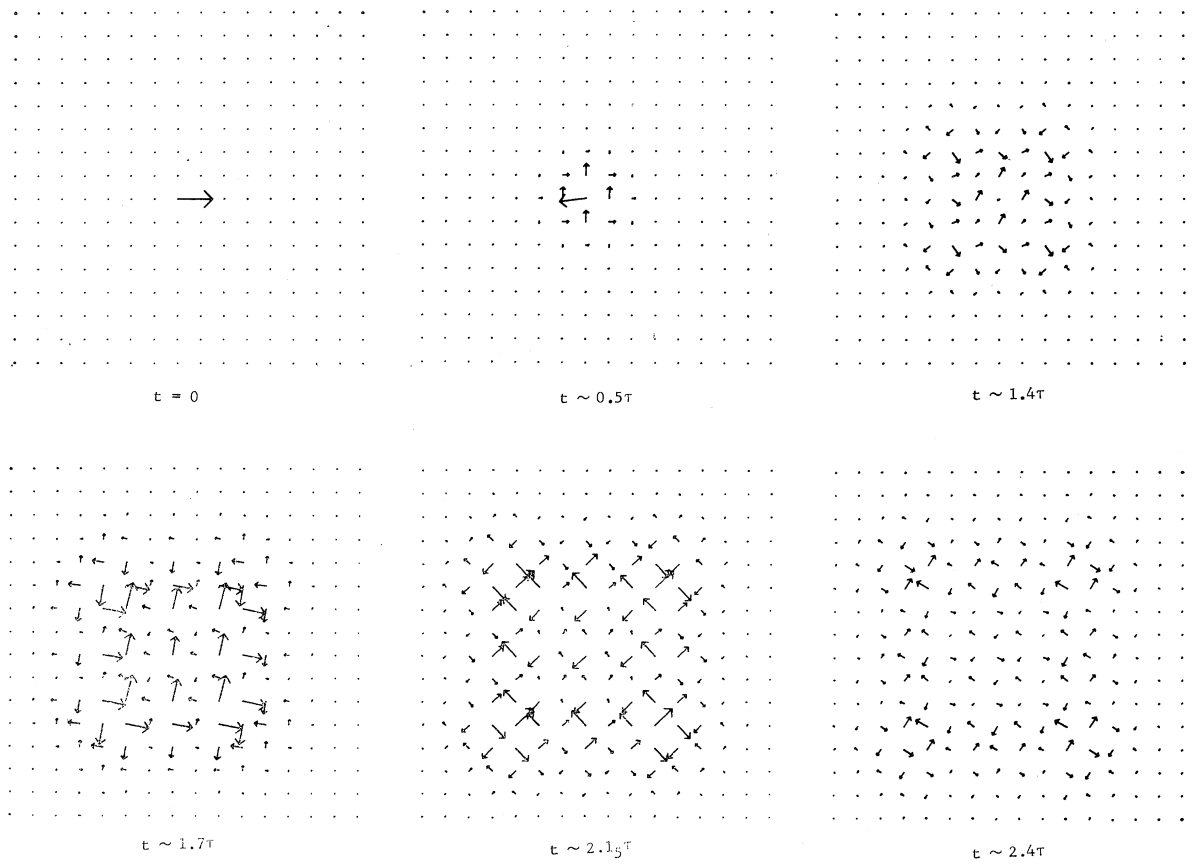

FIG. 14. A (100) planar section of a 16×16×16 spin array showing the disturbance (in x and y components of the spins) emanating from a single misaligned spin lying in the x direction (all others ferromagnetically in the z) at $t=0$.

[20] This noise might be overcome (or at least reduced) by averaging over many correlation-function samples. This was not done here, since the effort did not seem warranted.

employed is the precession time appropriate to total (i.e., $T=0$) magnetization. The main peak decays slowly with no hint of structure, within the scatter, in its tail. This is in agreement with Windsor's results, which displayed[21] no structure for infinite temperature. The [100] correlation function (not plotted) displays the main peak, with its maximum at $\tau=1$, and a similar smooth decay. Results obtained for more distant pairs display little above the noise. One obtains, from these results, a spin propagation velocity which is roughly half the value at $T=0$.

The suggestion of a characteristic spin-diffusion or group velocity was first raised by the results of Fig. 8. There was also some suggestion that this description oversimplifies the situation since structure was seen in the [$nn0$] and [nnn] functions at times less than the characteristic transit time of the "main"peak. A study of the spin diffusion associated with one displaced spin in an otherwise ferromagnetic array sheds some light on this. The evolution of such a system is displayed in Fig. 14. A spin at the center of a $16\times16\times16$ sample was initially pointed in the x direction; all others were ferromagnetically aligned in the z direction. The x and y components of a (100) plane of spins, including the displaced spin, are plotted in the figure as a function of time (note the factor of $7\frac{1}{2}$ change in scale between the second and third frames). Assuming a characteristic spin-diffusion or group velocity, one would expect a spherical wave front for the disturbances; in this plane it is square. Further samplings in the (110) plane (which we do not plot) show the disturbance to have a cubic wave front. The velocity of motion of the centers of this front is that already seen in Fig. 8. Such a result is not characteristic of a simple spin-diffusion process but it is consistent with the predictions of spin-wave theory for the case of one infinitesimally perturbed spin. Derivations, similar to those yielding Eq. (13) (see also Huber[13]), give

$$\langle \mathbf{S}_\perp{}^0(0)\cdot\mathbf{S}_\perp{}^{[hkl]}(\tau)\rangle \sim i^{h+k+l}J_h(\tfrac{1}{3}\tau)J_k(\tfrac{1}{3}\tau)J_l(\tfrac{1}{3}\tau)\,, \quad (23)$$

where the internal perturbation takes place at site 0 and at time $\tau=0$. The tendency to square wave fronts, the nodal lines, and the relative phases of 90° of adjacent spins which appear in Fig. 14 are consistent with this equation. The structure seen in the time-displaced correlations is thus predicted by spin-wave theory and it depends strongly on the topology of the simple cubic lattice [as manifested, for example, in the spin-wave dispersion curve, Eq. (8)]. The characteristic velocity seen in Fig. 8 is not simply that of a spin-diffusion process, and the structure which appears prior to the arrival of the main peak is to be expected.

[21] C. G. Windsor, Proc. Phys. Soc. (London) **91**, 353 (1967); see also C. G. Windsor, G. A. Briggs, and M. Kestigian, J. Phys. **C1**, 940 (1968).

ACKNOWLEDGMENTS

We would like to thank Miss E. Wolfson for assistance with the computer programming and G. A. Baker, M. E. Fisher, N. D. Mermin, P. C. Martin, P. Schofield, and S. A. Goudsmit for useful discussions.

PHYSICAL REVIEW VOLUME 181, NUMBER 2 10 MAY 1969

Temperature Dependence of the Susceptibility Tensor of a Weak Ferromagnet: $YFeO_3$†

G. Gorodetsky, S. Shtrikman, Y. Tenenbaum, and D. Treves
Department of Electronics, The Weizmann Institute of Science, Rehovot, Israel
(Received 28 October 1968)

The magnetic susceptibility of $YFeO_3$ has been measured in the temperature range 4.2–1000°K. The temperature dependence of the susceptibility is also derived theoretically using a Heisenberg Hamiltonian and applying the molecular-field approximation. In addition to nearest-neighbor isotropic exchange, antisymmetric exchange, and uniaxial anisotropy terms, a cubic anisotropy term is also included in the Hamiltonian in an attempt to account for the observed temperature variation of the susceptibility parallel to the antiferromagnetic axis. This model explains qualitatively the main features of the experimental results. Using the same model, the third-order term in the field dependence of the magnetization is calculated for $T=0$°K. It follows that, owing to the cubic anisotropy term, quantitative agreement is obtained with the observed departure from linearity in the field dependence of the magnetization, which was measured at 4.2°K and magnetic fields in the range 0–50 kOe.

I. INTRODUCTION

THE orthoferrites RFeO$_3$ (R is a rare earth or yttrium) belong to a class of weak ferromagnets with a slightly distorted perovskite crystallographic structure (space group $D_{2h}{}^{16}$–$Pbnm$).[1,2] The distortion from the ideal perovskite is mainly in the positions of the R^{3+} ions, while the environment of the Fe^{3+} ion remains essentially octahedral. Each unit cell contains

† Research sponsored in part by the Air Force Materials Laboratory Research and Technology Division AFSC through the European Office of Aerospace Research, U. S. Air Force, under Contract No. F61052-67C-0040.

[1] D. Treves, J. Appl. Phys. **36**, 1033 (1965); Phys. Rev. **125**, 1843 (1963), and references cited therein.
[2] M. Eibschütz, S. Shtrikman, and D. Treves, Phys. Rev. **156**, 562 (1967).